Impact of Turbulence in Long Range Quantum and Classical Communications

Ivan Capraro,[1] Andrea Tomaello,[1] Alberto Dall'Arche,[1] Francesca Gerlin,[1] Ruper Ursin,[2] Giuseppe Vallone,[1] and Paolo Villoresi[1,*]

[1]*Department of Information Engineering, University of Padova, via Gradenigo 6/B, 35131 Padova, Italy*
[2]*Institute for Quantum Optics and Quantum Information (IQOQI), Austrian Academy of Sciences, Boltzmanngasse 3, A-1090 Vienna, Austria*

(Received 30 July 2012; published 14 November 2012)

The study of the free-space distribution of quantum correlations is necessary for any future application of quantum and classical communication aiming to connect two remote locations. Here we study the propagation of a coherent laser beam over 143 km (between Tenerife and La Palma Islands of the Canary archipelagos). By attenuating the beam we also studied the propagation at the single photon level. We investigated the statistic of arrival of the incoming photons and the scintillation of the beam. From the analysis of the data, we propose the exploitation of turbulence to improve the signal to noise ratio of the signal.

DOI: 10.1103/PhysRevLett.109.200502 PACS numbers: 03.67.Hk, 42.50.Ar, 42.68.Bz, 92.60.Ta

Introduction.—The study of the free-space propagation of quantum correlations is necessary for any future application of quantum communication aiming to connect two remote locations. The problem related to the free-space propagation is represented by the atmospherical turbulence that acts as a temporal and spatial variation of the air refraction index. A turbulent channel acts as an increment of the losses on the transmitted photons due to beam wandering of the beam centroid or to scintillation, increasing the role of the noise [1–5]. The understanding of the propagation effects induced by turbulence at the receiver as well as the temporal statistics of the incoming photons is crucial to assess the quality of the communication and eventually the feasibility of the free-space ground-ground and space-ground links [6–8].

In this work we study the propagation of a free-space optical link (143 km) between Tenerife and La Palma Islands of the Canary archipelagos [9–11]. The transmitter is located at La Palma, on the roof of the Jacobus Kapteyn Telescope, and the receiver is the Optical Ground Station (OGS) at Tenerife. The campaign was performed during the nights between 17 and 25 September 2011.

Optical setup.—The optical setup of the transmitter is shown in Fig. 1. It consists of a suitably designed telescope whose key component is a singlet aspheric lens of 23 cm diameter and 220 cm focal length at 810 nm. The lens diameter was chosen to be significantly greater than the estimated Fried parameter r_0 [12] in order to obtain at the OGS a beam whose spot is comparable to the telescope primary mirror and consequently enhance the power transfer between the two sites. Our light source is an infrared (IR) diode at 808 nm coupled into a single mode fiber with an output power of about 6 mW and suitable attenuators. In order to facilitate the raw pointing, a mechanical XY stage has been added (we define the Z direction as the optical axis of the system). This stage moves all the 2.5 m long telescope in the XY plane. All the structure is assembled by three aluminum flanges; one holds the lens and one the focal plane, and the other is attached to the XY back stage. The lens is fixed to an articulated mount to prevent bending of the structure.

The IR source has been aligned by means of a dichroic mirror (DM) reflecting the 808 nm radiation. The platform carrying the focusing lens, the collimating lens, and the fiber port for the IR can be moved by a micrometric XYZ system based on stepped motors. In this way, the beam can be slightly steered by moving the focal spot at the singlet focus. The instantaneous deviation from the initial pointing direction is acquired by using a 532 nm beacon beam sent from the receiver by using a small portable low power laser module directly pointed towards La Palma without any optics. The beacon laser is acquired with a complementary metal oxide semiconductor camera placed on the movable platform after the DM transmission. The centroid of the

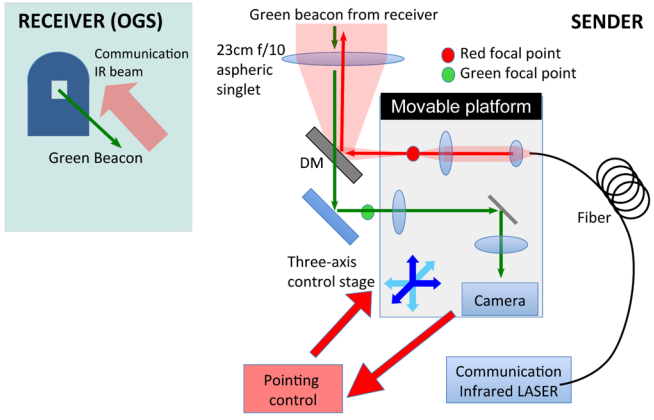

FIG. 1 (color online). Schematic of the optical setup. DM: dichroic mirror.

 © 2012 American Physical Society

beacon spot on the camera determines the correction on the outcoming IR laser by means of an error signal with respect to the reference position. The position of the spot at the camera is sampled about once a second and averaged for a number of frames; these data feed a control software that calculates the movement for the fine XY stage in order to compensate slow drift in the beam direction.

We collected data at the OGS in Tenerife in order to measure the received power and the scintillation and analyze the temporal structure of the signal. We placed in the OGS Coudè focus a photodiode and a power meter, and, when the beam is suitably attenuated at the transmitter with a neutral filter, we also collected data at the receiver with a single photon (Excelitas SPCM-AQRH model) detector (SPAD). The following data were recorded during the nights between 21 and 24 September 2011. We obtained an average attenuation of about 30 dB for many times during the best run with peaks of 27 dB averaged over 2 min. The attenuation is calculated from the fiber and not from the singlet lens: The attenuation of the telescope is thus included in the measured attenuation.

Link analysis.—Let us first describe the single photon detection acquisition. We performed several measurements by setting the counting interval T to 0.1, 1, and 10 ms. Because of turbulence effects, the mean photon number q in a counting interval at the receiver should follow a lognormal probability distribution [13]:

$$P(q) = \frac{1}{q\sqrt{2\pi\sigma^2}} e^{-[(\ln(q/\langle q\rangle)+(1/2)\sigma^2)]^2/(2\sigma^2)}, \qquad (1)$$

where $\langle q\rangle$ is the average, $\sigma^2 = \ln(1 + \mathrm{SI})$, and $\mathrm{SI} = \frac{\Delta q^2}{\langle q\rangle^2}$ is the scintillation index. If the counting interval T is large compared with the coherence time of the source and T is short compared with the turbulence time scale, the probability of detecting an n photon in each interval follows the Mandel distribution:

$$p_n = \int dq \frac{q^n e^{-q}}{n!} P(q). \qquad (2)$$

Note that the mean number of detected photons is $\langle n\rangle = \sum_n n p_n = \langle q\rangle$. We report the analysis of the temporal distribution of an acquisition with 1 ms counting interval in Fig. 2 (top). It is possible to observe that, when the average number of detected photons $\langle n\rangle$ is large (typically larger than 50) and the scintillation index bigger than 1, the lognormal and Mandel distribution are quite similar. Given the experimental scintillation as 2.23 ± 0.01 and the mean value of detected photons as 234, we show the counting occurrences together with the corresponding lognormal distribution in Fig. 2 (bottom). For comparison, we also insert the corresponding Mandel distribution with the $\langle q\rangle = 234.1 \pm 0.1$ and $\sigma = 349.2 \pm 0.2$ parameter obtained from the raw data. We evaluated the similarity between the experimental data and the lognormal or the Mandel curve, defined as $S = [(\sum \sqrt{p_i q_i})^2]/(\sum p_i \sum q_j)$,

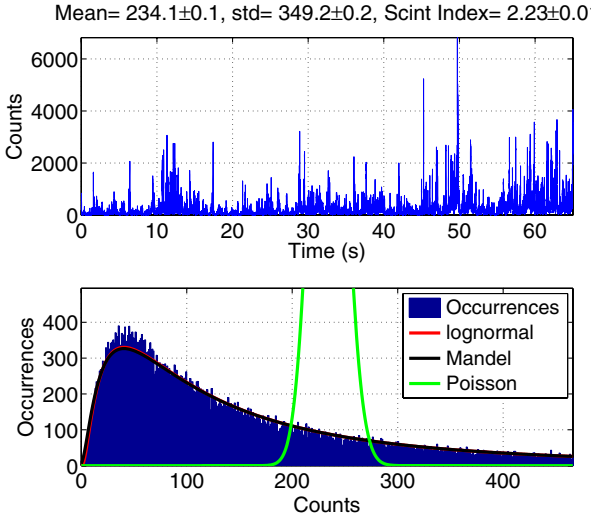

FIG. 2 (color online). SPAD temporal distribution of count occurrences and corresponding lognormal and Mandel curves. We can compare the data with the corresponding Poissonian distribution with the same mean value (234.1 ± 0.1) that would be obtained without turbulence.

where p_i and q_i are, respectively, the theoretical and experimental occurrence. The similarity of the lognormal curve with the data is 0.9959, while the Mandel curve has a similarity of 0.9967 showing clear evidence of the statistic transformation. The green curve represents the corresponding Poisson distribution with the same observed mean value, to compare what would have been obtained if the statistic of the arrival photon were purely Poissonian. In Table I, we report the data obtained for several different SPAD acquisitions.

As mentioned, we also measure the intensity of received light with a fast photodiode by using an intense laser source. In Fig. 3, we plot the temporal distribution of the photodiode voltage of a data set covering 20 s. The intensities are recorded with 50 kHz frequency. Also in this case the intensity occurrences follow a lognormal distribution (1) as shown from the lognormal curve with a similarity of 0.9896. In this case, the scintillation index evaluated from the experimental data is $\mathrm{SI} = \frac{\Delta I^2}{\langle I\rangle^2} = 1.19 \pm 0.01$.

Improving the SNR.—For both quantum and classical communication, it is of paramount importance to achieve a high signal to noise ratio (SNR). If a qubit state $|\psi\rangle$ encoded in the photon polarization must be sent between two remote locations, it is possible to determine the effect of (white) noise on the polarization fidelity [14]. Let us measure the SNR in dB, namely, $\mathrm{SNR} = 10\log_{10}\frac{N_s}{N_n}$, where N_n is the average amount of noise (coming from dark detections or background radiation) and N_s is the average number of detected photons. It is easy to show that the fidelity depends on the SNR as

$$F = 1 - \frac{1}{2(10^{\mathrm{SNR}/10})}. \qquad (3)$$

TABLE I. Data obtained for different single photon acquisition compared to the background (first line). For each acquisition we report the total duration of the acquisition (Time), the temporal windows defining the counting interval (Window), the mean number of counts in the counting interval (Mean), and its the standard deviation (Std). We also report the scintillation index (SI) and the frequency bound defined in such a way that all the frequencies below the bound contribute to 95% of the scintillation index (Bound). With High (Low) we indicate acquisition with a high (low) mean photon number detected during 1 s. We notice that for the last two data sets the bound is higher due to the low signal compared to the background (having a flat frequency spectrum).

	Mean	Std	Time (s)	Window (ms)	SI	Bound (Hz)
Backgr.	0.4732	0.7256	10	1	2.3515	475
Hi	5291	9135	650	10	2.9805	22
Hi	678.7	820.8	65	1	1.4626	43
Hi	510.4	751.9	65	1	2.1704	45
Hi	781.5	951.9	65	1	1.4834	42
Hi	180.2	312.0	65	1	2.997	39
Hi	234.1	349.2	65	1	2.2251	51
Hi	43.18	48.76	6.5	0.1	1.2748	81
Hi	21.17	26.34	6.5	0.1	1.5485	88
Hi	75.37	132.10	6.5	0.1	3.072	35
Hi	59.97	105.01	6.5	0.1	3.0659	37
Low	37.86	48.42	200	10	1.6355	35
Low	20.83	24.18	200	10	1.3479	35
Low	2.862	3.795	65	1	1.7578	384
Low	5.267	7.519	65	1	2.0383	258

In fact, since the background photons are completely depolarized, the received quantum state can be written as $\rho = \frac{N_s - N_n}{N_s} |\psi\rangle\langle\psi| + \frac{N_n}{N_s} \frac{\mathbb{1}}{2}$.

In order to improve the SNR for the transmission of single photons in a long distance free-space link as the present one, which uses a 1 m optical receiver, out of our findings we envisage the exploitation of the following procedure. With a given frequency (slower than the single photon transmission rate), the free-space channel is probed by means of a classical signal that gives the information of the instantaneous transmission of the channel. Only if the transmission is above a given threshold is the single photon signal acquired. It is crucial for the protocol to be efficient to correctly identify the "probing" frequency and the threshold to be used. This technique can also be used in the classical case, for instance, in on-off keying.

We report in Fig. 4 the frequency spectrum and the cumulative power spectrum of the data plotted in Fig. 2. The normalized plot of the power spectrum is obtained by normalizing the intensities by the average $I' = I/\langle I \rangle$. The power spectrum is related to the scintillation index as follows. We write the set of (normalized) acquisitions as I'_k with $k = 0, \ldots, N-1$ and $N = 20\ \mathrm{s}/20\ \mu\mathrm{s} = 10^6$ the

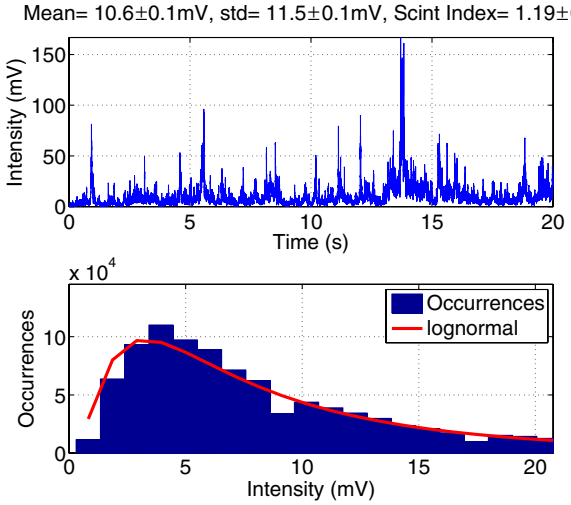

FIG. 3 (color online). Photodiode temporal distribution intensity occurrences and corresponding lognormal curve.

number of intensity acquisitions over 20 s. The Fourier components are given by $\tilde{I}_n = \sum_k I'_k \omega^{nk}$ with $\omega = e^{-(2\pi i/N)}$. By Parseval's theorem it is easy to show that $\mathrm{SI} = \frac{2}{N^2} \sum_{n=1}^{N/2} |\tilde{I}_n|^2$; namely, it is the cumulative power spectrum without the zero frequency ($\tilde{I}_0$) component. We can notice that the frequencies contributing to the scintillation (up to 95%) are within (almost) 50 Hz. For frequencies above around 500 Hz, the spectrum becomes flat, indicating that at this frequency the random noise is dominant. The typical fluctuations of the transmission channel due to turbulence are within 100 Hz (see Table I). The frequency analysis of the temporal scintillation indicates that the probing frequency does not need to be higher than 1 KHz.

In order to obtain further evidence, we analyzed the features of the counts above a given threshold of the signal

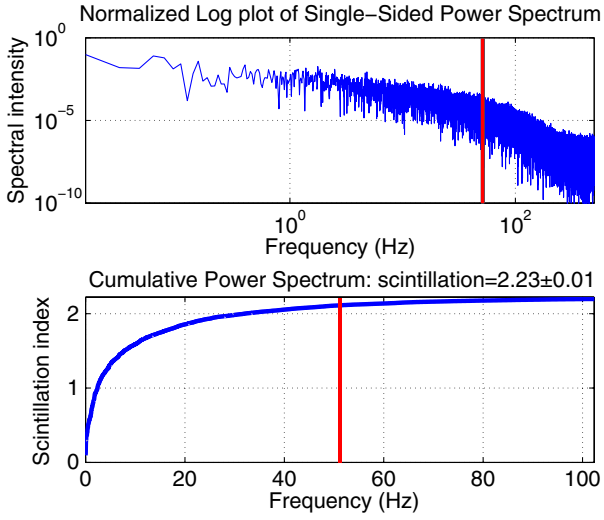

FIG. 4 (color online). SPAD power spectrum and cumulative power spectrum. Frequency bound (red vertical line): The frequencies below 51 Hz contribute to 95% of the scintillation index.

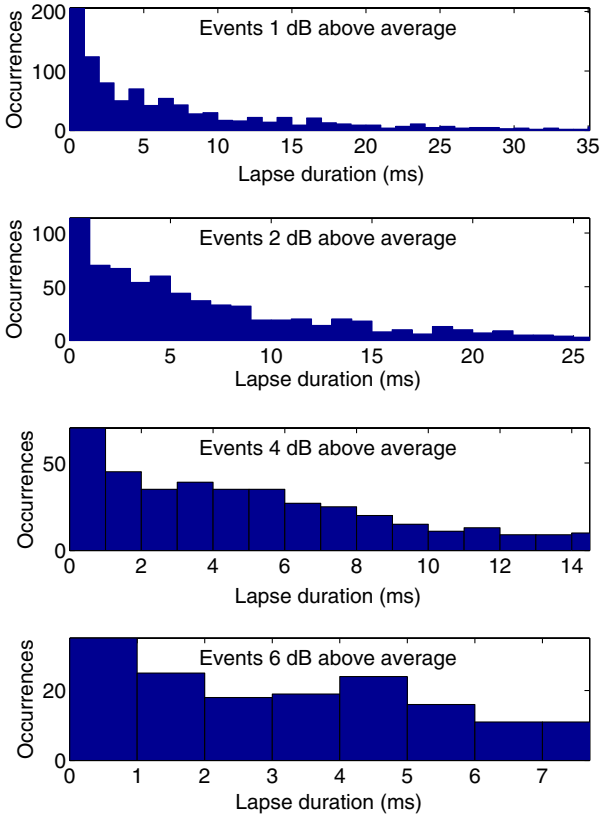

FIG. 5 (color online). Duration (in milliseconds) of events with overthreshold counting. In the different plots we considered a threshold of 1, 2, 4, and 6 dB above the average.

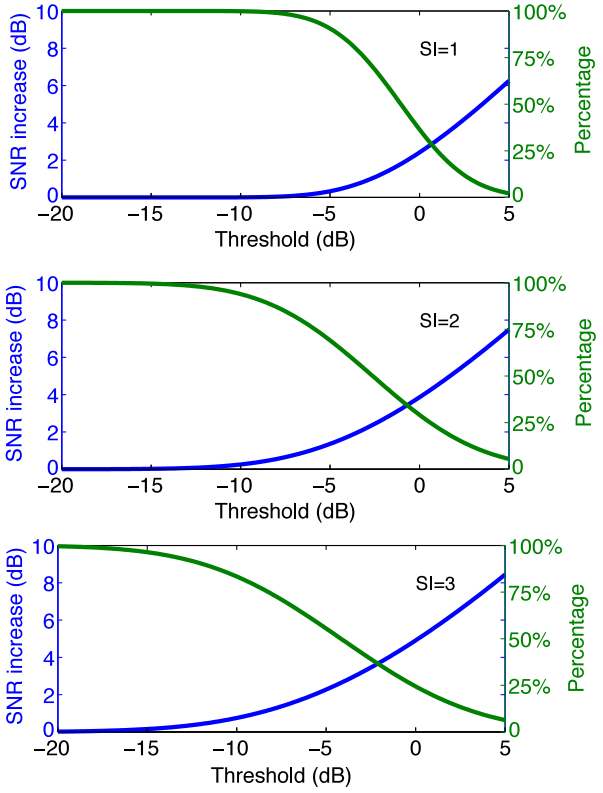

FIG. 6 (color online). SNR and the percentage of the overall counts that will be detected in the function of the threshold selection.

reported in Fig. 2. By considering a threshold of 1, 2, 4, and 6 dB above the average, we considered the duration (in milliseconds) of events with overthreshold counting. The results are shown in Fig. 5. The probability of obtaining an event above a given threshold q_0 can be predicted from the lognormal distribution [15]

$$p(q > q_0) = \frac{1}{2} - \frac{1}{2}\,\mathrm{erf}\left[\frac{\ln\frac{q_0}{\langle q\rangle} + \frac{1}{2}\sigma^2}{\sqrt{2\sigma^2}}\right], \tag{4}$$

where $\mathrm{erf}(x)$ is the Gaussian error function $\mathrm{erf}(x) = (2/\sqrt{\pi})\int_0^x e^{-t^2}dt$. Acquiring the single photon channel only if the probed transmission is above a given threshold implies an increase of the average photon counts in each time slot. It is possible to show that, by considering only the events in which the transmission satisfy $T > T_0$, the new mean value $\langle n\rangle_{\mathrm{thres}}$ is

$$\frac{\langle n\rangle_{\mathrm{thres}}}{\langle n\rangle} = \frac{1 - \mathrm{erf}\left[\frac{\ln\frac{T_0}{\langle T\rangle} - \frac{1}{2}\sigma^2}{\sqrt{2\sigma^2}}\right]}{1 - \mathrm{erf}\left[\frac{\ln\frac{T_0}{\langle T\rangle} + \frac{1}{2}\sigma^2}{\sqrt{2\sigma^2}}\right]} > 1. \tag{5}$$

Clearly, this threshold selection increases the SNR but at the same time decreases the overall counts in a given time. In Fig. 6, we show the increase (in decibels) of the SNR and the percentage of the overall counts that will be detected. In cases of strong turbulence and high noise, this technique could help the qubit transmission by "exploiting turbulence," namely, considering only the particular moments in which the turbulence increases the channel transmission.

In conclusion, the statistic of arrival of single photons over a free-space 143 km optical link has been analyzed, demonstrating the transformation from Poissonian to lognormal distribution and thus expanding this investigation for more than an order of magnitude in length with respect to previous results [13]. The evidence of consecutive subintervals of low losses allows us to envisage the exploitation of turbulence as an SNR improvement technique.

The authors wish to warmly thank for the help provided by Z. Sodnik of the European Space Agency and by C. Barbieri and S. Ortolani of University of Padova as well as by the Instituto de Astrofisica de Canarias (IAC), and in particular F. Sanchez-Martinez, A. Alonso, C. Warden and J.-C. Perez Arencibia, and by the Isaac Newton Group of Telescopes (ING), and in particular M. Balcells, C. Benn, J. Rey, A. Chopping, and M. Abreu. This work has been carried out within the Strategic-Research-Project QUINTET of DEI-University of Padova and the Strategic-Research-Project QUANTUMFUTURE of the University of Padova.

*Corresponding author.
paolo.villoresi@dei.unipd.it

[1] V. I. Tatarski, *Wave Propagation in a Turbulent Medium* (McGraw-Hill, New York, 1961).
[2] R. L. Fante, Proc. IEEE **63**, 1669 (1975).
[3] R. Fante, IEEE Trans. Antennas Propag. **23**, 382 (1975).
[4] R. L. Fante, Proc. IEEE **68**, 1424 (1980).
[5] F. Dios, J. A. Rubio, A. Rodríguez, and A. Comerón, Appl. Opt. **43**, 3866 (2004).
[6] P. Villoresi, T. Jennewein, F. Tamburini, M. Aspelmeyer, C. Bonato, R. Ursin, C. Pernechele, V. Luceri, G. Bianco, A. Zeilinger, and C. Barbieri, New J. Phys. **10**, 033038 (2008).
[7] C. Bonato, A. Tomaello, V. Da Deppo, G. Naletto, and P. Villoresi, New J. Phys. **11**, 045017 (2009).
[8] E. Meyer-Scott, Z. Yan, A. MacDonald, J.-P. Bourgoin, H. Hübel, and T. Jennewein, Phys. Rev. A **84**, 1 (2011).
[9] R. Ursin, S. Backus, H. C. K. F. Tiefenbacher, T. Schmitt-Manderbach, H. Weier, T. Scheidl, M. Lindenthal, B. Blauensteiner, T. Jennewein, J. Perdigues, P. Trojek *et al.*, Nat. Phys. **3**, 481 (2007).
[10] A. Fedrizzi, R. Ursin, T. Herbst, M. Nespoli, R. Prevedel, T. Scheidl, F. Tiefenbacher, T. Jennewein, and A. Zeilinger, Nat. Phys. **5**, 389 (2009).
[11] T. Scheidl, R. Ursin, J. Kofler, S. Ramelow, X.-S. Ma, T. Herbst, L. Ratschbacher, A. Fedrizzi, N. K. Langford, T. Jennewein, and A. Zeilinger, Proc. Natl. Acad. Sci. U.S.A. **107**, 19 708 (2010).
[12] D. L. Fried, J. Opt. Soc. Am. **56**, 1372 (1966).
[13] P. W. Milonni, J. H. Carter, C. G. Peterson, and R. J. Hughes, J. Opt. B **6**, S742 (2004).
[14] If $|\psi\rangle$ is the polarization state of the sent photon and ρ is the polarization density matrix of the received photon, the fidelity $F = \langle\phi|\rho|\phi\rangle$ is the probability of receiving the correct state.
[15] Here we replaced the Mandel distribution with the log-normal distribution.